Published in final edited form as:
Am J Physiol Heart Circ Physiol. 2008 May ; 294(5): H2400–H2405. doi:10.1152/ajpheart.01158.2007.

Locations of ectopic beats coincide with spatial gradients of NADH in a regional model of low-flow reperfusion

Matthew Kay[1,2], **Luther Swift**[1], **Brian Martell**[1], **Ara Arutunyan**[1], and **Narine Sarvazyan**[1]

[1] Department of Pharmacology and Physiology, The George Washington University, Washington DC

[2] Department of Electrical and Computer Engineering, The George Washington University, Washington DC

Abstract

We studied the origins of ectopic beats during low-flow reperfusion after acute regional ischemia in excised rat hearts. The left anterior descending coronary artery was cannulated. Perfusate was delivered to the cannula using an high-performance liquid chromatography pump. This provided not only precise control of flow rate but also avoided mechanical artifacts associated with vessel occlusion and deocclusion. Optical mapping of epicardial transmembrane potential served to identify activation wavefronts. Imaging of NADH fluorescence was used to quantify local ischemia. Our experiments suggest that low-flow reperfusion of ischemic myocardium leads to a highly heterogeneous ischemic substrate and that the degree of ischemia between adjacent patches of tissue changes in time. In contrast to transient ectopic activity observed during full-flow reperfusion, persistent ectopic arrhythmias were observed during low-flow reperfusion. The origins of ectopic beats were traceable to areas of high spatial gradients of changes in NADH fluorescence caused by low-flow reperfusion.

Reperfusion arrhythmias in clinical settings are considered to be relatively transient and benign, particularly if the heart is structurally intact. This is because restoration of blood flow to reversibly damaged tissue quickly reinstates the ionic balance across the cell membrane and, consequently, normal conduction resumes. However, in some situations (i.e., a partially resolved blood clot, unsuccessful angioplasty, or the incomplete dilation of a coronary artery following a spasm), flow to the ischemic area is only partially restored. Indeed, an estimate based on Pouiselle's law of laminar flow predicts that a 50% reduction in a vessel's radius will result in a flow rate that is 6% of its original value. Low-flow reperfusion may also happen during cardiopulmonary resuscitation(29).

While providing tissue with minimal nutrients, low-flow reperfusion could be more arrhythmogenic than either ischemia or full-flow reperfusion. During low-flow reperfusion of an ischemic tissue bed, one can envision a continuously shifting pattern of flows between downstream vessels. This could be the result of autoregulation caused by ischemia-induced relaxation of smooth muscle cells, which increases the diameter of small coronary arteries, resulting in increased flow rates. Alternatively, it could be due to local hyperemia as adjacent tissue beds compete for the limited amount of flow. As a result of local shifts in flow, reperfused patches of myocardium might act as a substrate for persistent ectopic beats via calcium-overload mechanisms(2,21). The effects of reperfusion-induced calcium

Address for reprint requests and other correspondence: N. Sarvazyan, Dept. of Pharmacology and Physiology, 2300 Eye St., Washington NW DC 20037 (phynas@gwumc.edu).

overload can be further amplified by the release of norepinephrine from ischemic nerve endings(2,15,41).

The goal of our studies was to obtain direct experimental evidence for an increased incidence of ectopic beats during low-flow reperfusion. To avoid mechanical artifacts associated with vessel occlusion and deocclusion we remotely controlled flow to the left anterior descending coronary artery (LAD) by cannulating the vessel and delivering perfusate with an high-performance liquid chromatography (HPLC) pump. We imaged epicardial NADH fluorescence to measure local levels of ischemia. In parallel, transmembrane potentials were optically mapped to visualize activation wave fronts. A bipolar epicardial electrogram was recorded to continuously monitor heart rate. Data were analyzed to determine the incidence of arrhythmias and to reveal sources of ectopic beats.

In agreement with earlier studies (11,14,31), full-flow reperfusion of regionally ischemic myocardium was associated with brief arrhythmic episodes, which consisted of transient ectopic beats and occasional short-lived reentries. In contrast, we found that low-flow reperfusion of regionally ischemic myocardium led to persistent arrhythmias. These arrhythmias were fueled by multiple ectopic beats that were generated within areas having the highest spatial gradients of changes in NADH.

METHODS

Hearts from male Sprague-Dawley rats (300–400 g) were excised and Langendorff-perfused with oxygenated Tyrode solution. The LAD was cannulated with polyimide tubing (127 μm ID), just distal to the coronary ostium (Fig. 1*B*). This is a technique we call “microcannulation.” With microcannulation, the flow of perfusate to a specific left ventricular myocardial volume was precisely controlled. The microcannula was connected to an HPLC pump (Series I, Scientific Systems) to deliver perfusate at 2.00 ml/min, the nominal flow rate. Perfusate was delivered to the right ventricle, septum, and any branches of the left coronary artery above the site of cannulation by perfusing the aorta at constant pressure (60 mmHg), as shown in Fig. 1*C*. A representative border between the tissue fed by the coronary ostia and the LAD cannula is shown in Fig. 1*A*. Intrinsic heart rate (~30–90 beats/min) was stable throughout the experiment, unless arrhythmia was induced by reperfusion or other intervention. A detailed description of the microcannulation technique can be found in a separate technical report(37). All procedures involving animals have been approved by the Institutional Animal Care and Use Committee.

Hearts were stained with the potentiometric dye RH237 (10 μM solution, Molecular Probes), of which bolus injections (5 ml) were delivered to the aorta and the LAD. To prevent motion artifact Blebbistatin (10 μM) was added to the perfusate (13). After a stabilization period of 15–20 min, regional ischemia was induced by turning off the flow to the microcannula. The progression of ischemia was monitored at least every 2–3 min by imaging RH237 fluorescence for 12 s, followed by NADH imaging for 5 s. Flow to the LAD was resumed after 30 min of ischemia. A bipolar electrode was placed behind the heart to monitor basic electrical activity. Conclusions are based on a total of 15 successful microcannulation experiments, including 5 ischemia-full reperfusion experiments and 10 ischemia-low flow reperfusion studies. Typical electrograms, NADH, and transmembrane voltage data are shown.

An optical mapping system consisting of two CCD cameras (Andor IXON DV860s) fitted with a dual-port adapter (Andor CSU Adapter Dual Cam), a dichroic mirror (550 nm), and a single lens (Cosmicar 6 mm, F/1.0 with +27 closeup lenses) was used to image the epicardial fluorescence of RH237 and NADH from the same field of view. To record optical

action potentials the epicardium was illuminated using two light emitting diodes (LumiLEDs, 530/35 nm). The resulting fluorescence of RH237 was long pass filtered at 680 nm and recorded at 250 fps. To record NADH the epicardium was illuminated with ultraviolet light (<360 nm) from a 100-W mercury lamp (Zeiss HBO100 W/2). The resulting fluorescence of NADH was band-pass filtered (475/50 nm) and recorded using the second CCD camera.

RH237 fluorescence was processed (7) to subtract background fluorescence from each image, and signals for each pixel were normalized. Noise was reduced using a digital low-pass Butterworth filter (passband and stopband frequencies at 30 and 40 Hz, respectively), and fluorescence signals were smoothed using a spatiotemporal conical filter with a radius of three pixels. The progression of ischemia was monitored as the average level of NADH fluorescence within a region of interest.

Processed datasets of RH237 fluorescence were analyzed to record the location of ectopic beats. They were identified as wave fronts having a localized source within the ischemic bed. The center point of the initial rise of RH237 fluorescence for each ectopic beat was used to pinpoint its source. Center points that had the same pixel location were automatically eliminated in subsequent spatial analyses of ectopic sources. Typically, between 50 and 150 spatially unique ectopic sources (center points) were identified during 15 min of low-flow reperfusion.

Local changes in NADH fluorescence [dNADH(i, j), Eq. 1] were determined by subtracting an NADH image acquired immediately before initiating low-flow reperfusion [$\mathrm{NADH}_{\mathrm{before}}(i, j)$] from an NADH image acquired after low-flow reperfusion [$\mathrm{NADH}_{\mathrm{after}}(i, j)$]. The magnitude of the spatial gradient of dNADH [$|\nabla\ \mathrm{dNADH}(i, j)|$] was then computed using Eq. 2.

$$\mathrm{dNADH}(i, j)=\mathrm{NADH}_{\mathrm{after}}(i, j) - \mathrm{NADH}_{\mathrm{before}}(i, j) \tag{1}$$

$$|\nabla \mathrm{dNADH}(i, j)| = \sqrt{\left\{\frac{\mathrm{d}[\mathrm{dNADH}(i, j)]}{\mathrm{d}x}\right\}^2 + \left\{\frac{\mathrm{d}[\mathrm{dNADH}(i, j)]}{\mathrm{d}y}\right\}^2} \tag{2}$$

RESULTS

Epicardial NADH during acute regional ischemia and full-flow reperfusion

Epicardial NADH patterns before, during, and after acute regional ischemia for a typical experiment are shown in Fig. 2. A distinct area of elevated NADH fluorescence covered most of the left ventricle, as indicated by the white areas in Fig. 2*A*. Although the tissue bed perfused by the LAD was slightly different for each heart, the overall area and location was similar. The temporal progression of ischemia is shown in Fig. 2*B*. NADH levels steadily increased after the cessation of LAD flow, plateaued after 10.5 ± 0.9 min, and remained elevated until the reperfusion. The elevation of NADH was relatively uniform within the entire ischemic bed (Fig. 2*A*, *top row*). On the other hand, NADH during reperfusion was much more heterogeneous, with patches of tissue becoming less ischemic more rapidly than others (Fig. 2*A*, *bottom row*).

Ectopic beats during regional full-flow reperfusion

Full-flow reperfusion of regionally ischemic myocardium was associated with a short period of tachyarrhythmias, shown in Fig. 2*B* as a transient peak in average heart rate. The two cases illustrate the similarities and variability between individual hearts. The transient tachyarrhythmic episodes consisted of ectopic beats and occasional short-lived reentries. A majority of the ectopic beats were traceable to the border area, in agreement with previous studies (31). An example of a reperfusion-induced propagation disturbance is shown in Fig. 2*C*. The top row shows a nominal beat and the bottom two rows illustrate the transition from ectopic activity to reentry.

Heart rate and spatial gradients of changes of NADH fluorescence caused by low-flow reperfusion

Low-flow reperfusion (0.20 ml/min) of regionally ischemic myocardium caused sustained periods of tachyarrhythmias (Fig. 3*A*). The spatial heterogeneity of NADH fluorescence increased during low-flow reperfusion (Fig. 3*B*). Notably, NADH fluorescence decreased in some regions, whereas in other regions it increased or changed very little (Fig. 3*C*). The spatial gradient of changes in NADH fluorescence was computed to identify boundaries between tissue regions with different degrees of reflow as described in METHODS. An example of dNADH and the corresponding |∇dNADH| image as a pseudocolored surface is shown in Fig. 4*A*, *right* and *left* panels, respectively.

Local changes and spatial gradients of NADH at ectopic sources

Temporal changes and the spatial gradients of NADH fluorescence in the vicinity of each ectopic source were analyzed to reveal whether the location of ectopic sources was determined by the change in the NADH in time or time and space (Fig. 4*A*). NADH levels changed over several minutes (Fig. 3*C*), whereas ectopic beats from individual sources appeared much more rapidly (within seconds). Because of this, sites of multiple ectopic sources could be superimposed with one image of dNADH (Fig. 4*A*). A visual analysis of the sites of ectopic sources combined with NADH data (red dots plotted with dNADH and black dots plotted with |∇dNADH|, Fig. 4*A*) suggested a strong correlation between ectopic locations and the spatial gradient of dNADH. A detailed statistical analysis was used to confirm this conclusion. First, dNADH and |∇dNADH| maps were spatially smoothed by averaging values within a 2.5-pixel radius at each pixel. Next, two sets of dNADH and |∇dNADH| values were analyzed: one set contained those values at sites of ectopic sources (*set A*), and another set contained those values for a uniformly distributed set of random sites (*set B*). *Set B* equaled in number to *set A*. Nonpaired *t*-tests and Kolmogorov-Smirnov nonparametric tests were used to examine the null hypothesis that there was no difference between dNADH and |∇dNADH| in *sets A* and *B*. The means of dNADH, |∇dNADH|, and their histograms are shown in Fig. 4, *B* and *C*, for sets *A* (ectopic sites), *B* (random sites), and *C* (all sites) from two representative studies. We found that dNADH was not significantly different between ectopic sites and random sites. However, |∇dNADH| was highly significantly different between ectopic sites, random sites, and all sites ($P < 1.0e^{-5}$).

DISCUSSION

To the best of our knowledge this is the first study that has employed high-resolution optical mapping of NADH and transmembrane potential to correlate sites of ectopic beats with the underlying spatial distribution and degree of acute ischemia. This was accomplished by controlling flow to the LAD to mimic low-flow reperfusion. The technique allowed mechanical artifacts associated with vessel occlusion and de-occlusion to be avoided, which was essential for mapping the exact locations of ectopic sources. As such, our studies provide the first intact-heart optical mapping recordings of ectopic beats originating from

regionally ischemic and reperfused tissue. Zaitsev et al. (40) have described wave-break formation during ventricular fibrillation in regionally ischemic pig hearts, but they did not study reperfusion arrhythmias. Other studies have only used optical mapping to describe activity during global ischemia and/or global reperfusion (18,24,25,38) or in heart preparations with healed infarcts (28).

Many mechanistic insights of reperfusion arrhythmias have been provided by earlier studies using multielectrode recordings, biochemical assessment, or both (5,11,14,20,22,39). Acute ischemia results in acute biochemical changes, including acidification, accelerated efflux of intracellular potassium, accumulation of acyl-carnitines, and lysophospholipids (9,12,19,26). The ensuing depolarization of resting membrane potentials, slowing of conduction, and increased dispersion of refractoriness all contribute to reentrant arrhythmias, which are prevalent during the first phase (1a) of an ischemic episode (19,20,27). This phase is followed by a short period when arrhythmia occurrence diminishes, likely due to the diffusion of K^+ from the occluded area and the release of endogenous catecholamines, which temporarily improve tissue conductivity and excitability (9,30). This is followed by phase 1b (20), during which a second rise of K^+ occurs, gap junctional coupling decreases, and catecholamine-mediated triggered activity via delayed afterdepolarizations leads to an increased incidence of ectopic arrhythmias (10,17,23,27,30,36). If the occlusion persists, irreversible cell injury ensues and is associated with progressive cell uncoupling, calcium overload, and cell death (8,9,23). Reperfusion of ischemic myocardium leads to a high incidence of arrhythmias, mostly via nonreentrant mechanisms (32,34) with intracellular calcium overload as the major culprit (3,9,21). Electrode mapping studies in open-chest canines have shown that during acute ischemia 25% and 75% of arrhythmias occurring during ischemia and reperfusion, respectively, can be traced to ectopic sources–with a majority located near ischemic border zones (10,33).

The data we have presented are in agreement with the findings described above, specifically with the transient nature of reperfusion arrhythmias (6), the localization of ectopic sources to ischemic boundaries (10,33), and heterogeneity of reflow during reperfusion(16). However, our main emphasis is not on additional evidence that confirms previously established ectopic and/or reentry-based ischemia-reperfusion events. Instead, we call attention to the marked difference in electrical activity between full-flow and low-flow reperfusion. Low-flow reperfusion and the resulting patterns of flow create, in effect, a continuous boundary between partially reperfused and ischemic tissue within an ischemic tissue bed. This fuels a persistent generation of ectopic beats during low-flow reperfusion, creating a highly arrhythmogenic substrate. These findings match our previous in vitro studies where we hypothesized that ectopic beats generated during ischemia could be caused by microreperfusion of the ischemic border zone (1,2,35). Such transient ectopic waves can later transition into longer-lived reentrant sources upon changes in cell-cell coupling, tissue excitability, or position of the boundary (4,35).

Limitations

Studies were performed using unloaded blood-free excised rat hearts that were perfused with Tyrode solution. Therefore, the direct applicability of our results to clinical cases is limited and additional studies are needed to fully translate the observed phenomena to human patients.

Acknowledgments

We thank Vishal Khatri for excellent technical assistance.

GRANTS

Financial support by the American Heart Association, Mid-Atlantic Affiliate (BGIA 0665377U to M. W. Kay) and the National Heart, Lung, Blood Institute (HL-076722 to N. Sarvazyan) is gratefully acknowledged.

References

1. Arutunyan A, Swift LM, Sarvazyan N. Initiation and propagation of ectopic waves: insights from an in vitro model of ischemia-reperfusion injury. Am J Physiol Heart Circ Physiol 2002;283:H741–H749. [PubMed: 12124223]
2. Arutunyan A, Pumir A, Krinsky VI, Swift LM, Sarvazyan N. Behavior of ectopic surface: effects of β-adrenergic stimulation and uncoupling. Am J Physiol Heart Circ Physiol 2003;285:H2531–H2542. [PubMed: 12893638]
3. Bers, DM. Optical Mapping of Cardiac Excitation and Arrhythmia. Dordrecht, The Netherlands: Kluwer Academic; 2001. Excitation-contraction coupling and cardiac contracttile force; p. 275-281.
4. Biktashev V, Arutunyan A, Sarvazyan N. Generation and escape of local waves from the boundary of uncoupled cardiac tissue. Biophys J. 2008 Jan 22; [Epub ahead of print].
5. Bricknell OL, Opie LH. Effects of substrates on tissue metabolic changes in the isolated rat heart during underperfusion and on release of lactate dehydrogenase and arrhythmias during reperfusion. Circ Res 1978;43:102–115. [PubMed: 207459]
6. Brooks WW, Conrad CH, Morgan JP. Reperfusion induced arrhythmias following ischaemia in intact rat heart: role of intracellular calcium. Cardiovasc Res 1995;29:536–542. [PubMed: 7796448]
7. Byrd IA, Kay MW, Pollard AE. Interactions between paced wavefronts and monomorphic ventricular tachycardia: implications for antitachycardia pacing. J Cardiovasc Electrophysiol 2006;17:1129–1139. [PubMed: 16989652]
8. Carmeliet E. Cardiac ionic currents and acute ischemia: from channels to arrhythmias. Physiol Rev 1999;79:917–1017. [PubMed: 10390520]
9. Cascio WE, Johnson TA, Gettes LS. Electrophysiologic changes in ischemic ventricular myocardium. I. Influence of ionic, metabolic, and energetic changes. J Cardiovasc Electrophysiol 1995;6:1039–1062. [PubMed: 8589873]
10. Coronel R, Wilms-Schopman FJ, Dekker LR, Janse MJ. Heterogeneities in [K+]o and TQ potential and the inducibility of ventricular fibrillation during acute regional ischemia in the isolated perfused porcine heart. Circulation 1995;92:120–129. [PubMed: 7788906]
11. Corr PB, Witkowski FX. Arrhythmias associated with reperfusion: basic insights and clinical relevance. J Cardiovasc Pharmacol 1984;6(Suppl 6):S903–S909. [PubMed: 6084147]
12. Corr PB, Yamada KA. Selected metabolic alterations in the ischemic heart and their contributions to arrhythmogenesis. Herz 1995;20:156–168. [PubMed: 7543431]
13. Fedorov VV, Lozinsky IT, Sosunov EA, Anyukhovsky EP, Rosen MR, Balke CW, Efimov IR. Application of blebbistatin as an excitation-contraction uncoupler for electrophysiologic study of rat and rabbit hearts. Heart Rhythm 2007;4:619–626. [PubMed: 17467631]
14. Ferrier GR, Moffat MP, Lukas A. Possible mechanisms of ventricular arrhythmias elicited by ischemia followed by reperfusion. Studies on isolated canine ventricular tissues. Circ Res 1985;56:184–194. [PubMed: 3971500]
15. Gyorke S, Gyorke I, Lukyanenko V, Terentyev D, Viatchenko-Karpinski S, Wiesner TF. Regulation of sarcoplasmic reticulum calcium release by luminal calcium in cardiac muscle. Front Biosci 2002;7:d1454–d1463. [PubMed: 12045014]
16. Hariman RJ, Louie EK, Krahmer RL, Bremner SM, Euler D, Hwang MH, Ferguson JL, Loeb HS. Regional changes in blood flow, extracellular potassium and conduction during myocardial ischemia and reperfusion. J Am Coll Cardiol 1993;21:798–808. [PubMed: 8436763]
17. Hill JL, Gettes LS. Effect of acute coronary artery occlusion on local myocardial extracellular K+ activity in swine. Circulation 1980;61:768–778. [PubMed: 7357719]
18. Huizar JF, Warren MD, Shvedko AG, Kalifa J, Moreno J, Mironov S, Jalife J, Zaitsev AV. Three distinct phases of VF during global ischemia in the isolated blood-perfused pig heart. Am J Physiol Heart Circ Physiol 2007;293:H1617–H1628. [PubMed: 17545483]
19. Janse MJ, Wit AL. Electrophysiological mechanisms of ventricular arrhythmias resulting from myocardial ischemia and infarction. Physiol Rev 1989;69:1049–1169. [PubMed: 2678165]

20. Kaplinsky E, Ogawa S, Balke CW, Dreifus LS. Two periods of early ventricular arrhythmia in the canine acute myocardial infarction model. Circulation 1979;60:397–403. [PubMed: 445757]
21. Karmazyn M, Gan XT, Humphreys RA, Yoshida H, Kusumoto K. The myocardial Na(+)-H(+) exchange: structure, regulation, and its role in heart disease. Circ Res 1999;85:777–786. [PubMed: 10532945]
22. Kerber RE, Marcus ML, Ehrhardt J, Wilson R, Abboud FM. Correlation between echocardiographically demonstrated segmental dyskinesis and regional myocardial perfusion. Circulation 1975;52:1097–1104. [PubMed: 1182955]
23. Kleber AG, Riegger CB, Janse MJ. Electrical uncoupling and increase of extracellular resistance after induction of ischemia in isolated, arterially perfused rabbit papillary muscle. Circ Res 1987;61:271–279. [PubMed: 3621491]
24. Lakireddy V, Baweja P, Syed A, Bub G, Boutjdir M, El-Sherif N. Contrasting effects of ischemia on the kinetics of membrane voltage and intracellular calcium transient underlie electrical alternans. Am J Physiol Heart Circ Physiol 2005;288:H400–H407. [PubMed: 15345492]
25. Lakkireddy V, Bub G, Baweja P, Syed A, Boutjdir M, El-Sherif N. The kinetics of spontaneous calcium oscillations and arrhythmogenesis in the in vivo heart during ischemia/reperfusion. Heart Rhythm 2006;3:58–66. [PubMed: 16399055]
26. McHowat J, Yamada KA, Wu J, Yan GX, Corr PB. Recent insights pertaining to sarcolemmal phospholipid alterations underlying arrhythmogenesis in the ischemic heart. J Cardiovasc Electrophysiol 1993;4:288–310. [PubMed: 8269301]
27. Menken U, Wiegand V, Bucher P, Meesmann W. Prophylaxis of ventricular fibrillation after acute experimental coronary occlusion by chronic beta-adrenoceptor blockade with atenolol. Cardiovasc Res 1979;13:588–594. [PubMed: 519661]
28. Mills WR, Mal N, Forudi F, Popovic ZB, Penn MS, Laurita KR. Optical mapping of late myocardial infarction in rats. Am J Physiol Heart Circ Physiol 2006;290:H1298–H1306. [PubMed: 16214848]
29. Paradis NA, Martin GB, Rivers EP, Goetting MG, Appleton TJ, Feingold M, Nowak RM. Coronary perfusion pressure and the return of spontaneous circulation in human cardiopulmonary resuscitation. JAMA 1990;263:1106–1113. [PubMed: 2386557]
30. Penny WJ. The deleterious effects of myocardial catecholamines on cellular electrophysiology and arrhythmias during ischaemia and reperfusion. Eur Heart J 1984;5:960–973. [PubMed: 6442888]
31. Pogwizd SM, Corr PB. Electrophysiologic mechanisms underlying arrhythmias due to reperfusion of ischemic myocardium. Circulation 1987;76:404–426. [PubMed: 3608126]
32. Pogwizd SM, Corr B. The contribution of nonreentrant mechanisms to malignant ventricular arrhythmias. Basic Res Cardiol 1992;87:115–129. [PubMed: 1299206]
33. Pogwizd SM, Hoyt RH, Saffitz JE, Corr PB, Cox JL, Cain ME. Reentrant and focal mechanisms underlying ventricular tachycardia in the human heart. Circulation 1992;86:1872–1887. [PubMed: 1451259]
34. Pogwizd SM. Nonreentrant mechanisms underlying spontaneous ventricular arrhythmias in a model of nonischemic heart failure in rabbits. Circulation 1995;92:1034–1048. [PubMed: 7543829]
35. Pumir A, Arutunyan A, Krinsky V, Sarvazyan N. Genesis of ectopic waves: role of coupling, automaticity, and heterogeneity. Biophys J 2005;89:2332–2349. [PubMed: 16055545]
36. Smith, WTt; Fleet, WF.; Johnson, TA.; Engle, CL.; Cascio, WE. The Ib phase of ventricular arrhythmias in ischemic in situ porcine heart is related to changes in cell-to-cell electrical coupling. Experimental Cardiology Group, University of North Carolina. Circulation 1995;92:3051–3060. [PubMed: 7586276]
37. Swift L, Martell B, Khatri V, Arutunyan A, Sarvazyan N, Kay M. Controlled regional hypoperfusion in Langendorff heart preparations. Physiol Meas 2008;29:269–279. [Epub 2008 Feb 5]. [PubMed: 18256457]
38. Wu TJ, Lin SF, Hsieh YC, Ting CT, Chen PS. Ventricular fibrillation during no-flow global ischemia in isolated rabbit hearts. J Cardiovasc Electrophysiol 2006;17:1112–1120. [PubMed: 16879627]

39. Yamada KA, Saffitz JE, Corr PB. Role of α- and β-adrenergic receptor stimulation in the genesis of arrhythmias during myocardial ischaemia. Eur Heart J 1986;7(Suppl A):85–90. [PubMed: 2873040]

40. Zaitsev AV, Guha PK, Sarmast F, Kolli A, Berenfeld O, Pertsov AM, de Groot JR, Coronel R, Jalife J. Wavebreak formation during ventricular fibrillation in the isolated, regionally ischemic pig heart. Circ Res 2003;92:546–553. [PubMed: 12600877]

41. Zipes DP, Rubart M. Neural modulation of cardiac arrhythmias and sudden cardiac death. Heart Rhythm 2006;3:108–113. [PubMed: 16399065]

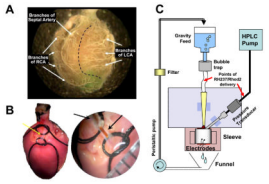

Fig. 1.

Microcannulation of the left anterior descending artery (LAD) of a rat heart. *A*: right and left coronary artery beds. Polymer casts show the main branches of the coronary circulation. A dotted line delineates two idealized perfusion zones: one fed by the coronary ostia (*left*) and another fed by the microcannula (*right*). RCA, right coronary artery. LCA, left coronary artery. *B*: isolation of the LAD for microcannulation. On the right, the tip of the microcannula is shown just before it is inserted into the LAD. *C*: schematics of a perfusion system used for optically mapping the heart.

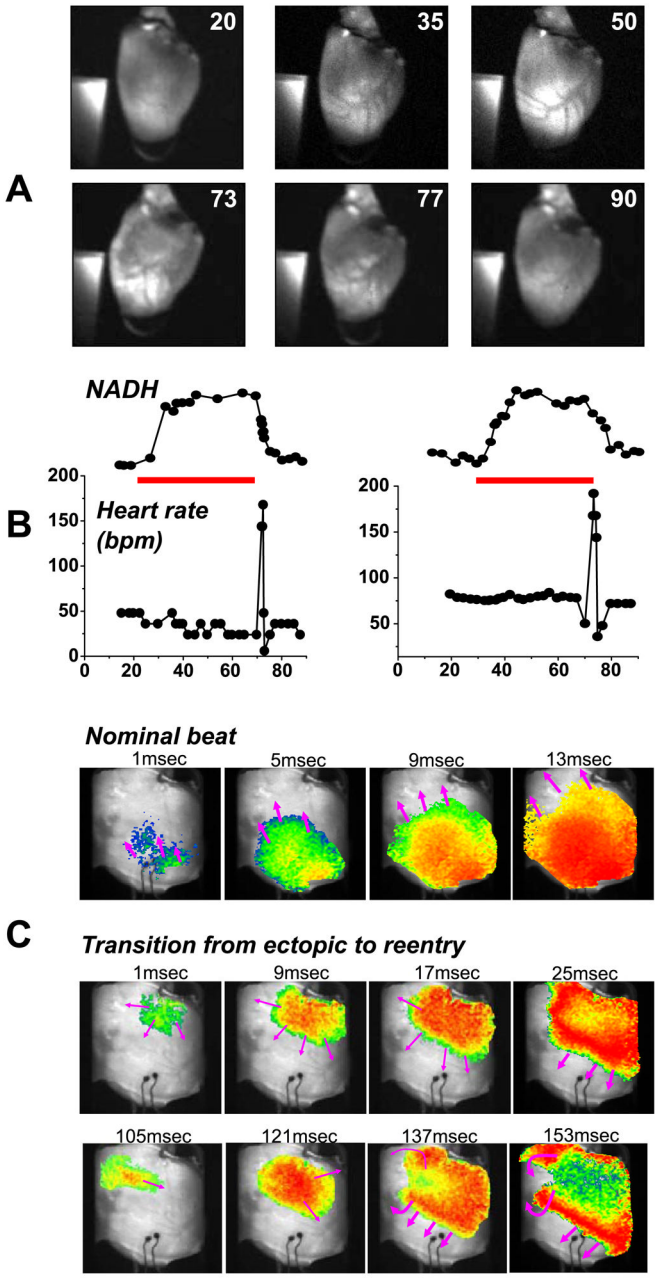

Fig. 2.

NADH fluorescence and heart rhythm during acute local ischemia and full-flow reperfusion. *A*: images of NADH fluorescence before, during, and after ischemia. Time (in minutes) from the start of the study is shown in top right corner of each image. A piece of uranyl glass is seen in each frame. Its fluorescence was used to normalize epicardial NADH fluorescence. *B*: average normalized NADH (*top*) is plotted with average heart rate (bpm, beats/min) (*bottom*) during local ischemia and full-flow reperfusion for two studies. The duration of regional ischemia is shown as a red bar. *C*: propagation of a wave front before the initiation of acute regional ischemia during the basic intrinsic rate (*top row*). Propagation of a wave front from a repetitive high-frequency ectopic beat during an arrhythmia induced by full-

flow reperfusion (*middle row*). Wave fronts caused by the transition from ectopic activation (*middle row*) to a repeating reentry (*bottom row*).

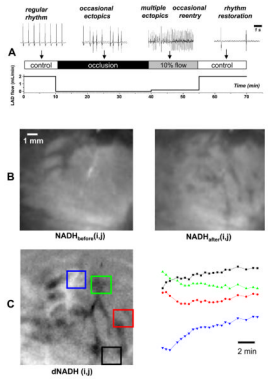

Fig. 3.

Changes in heart rate and epicardial NADH caused by low-flow reperfusion. *A*: bottom serves to illustrate low-flow reperfusion experiment. *Top traces* show representative epicardial electrograms from corresponding segments of the protocol. Note that the time scale for electrograms is different and is shown by a scale bar on the *top right. B: left*, NADH immediately before low-flow reperfusion; *right*, NADH after 13 min of low-flow reperfusion. *C: left*, dNADH obtained by subtracting the NADH images shown in *B; right*, average temporal changes of NADH induced by low-flow reperfusion for the four color-coded regions shown at *left*.

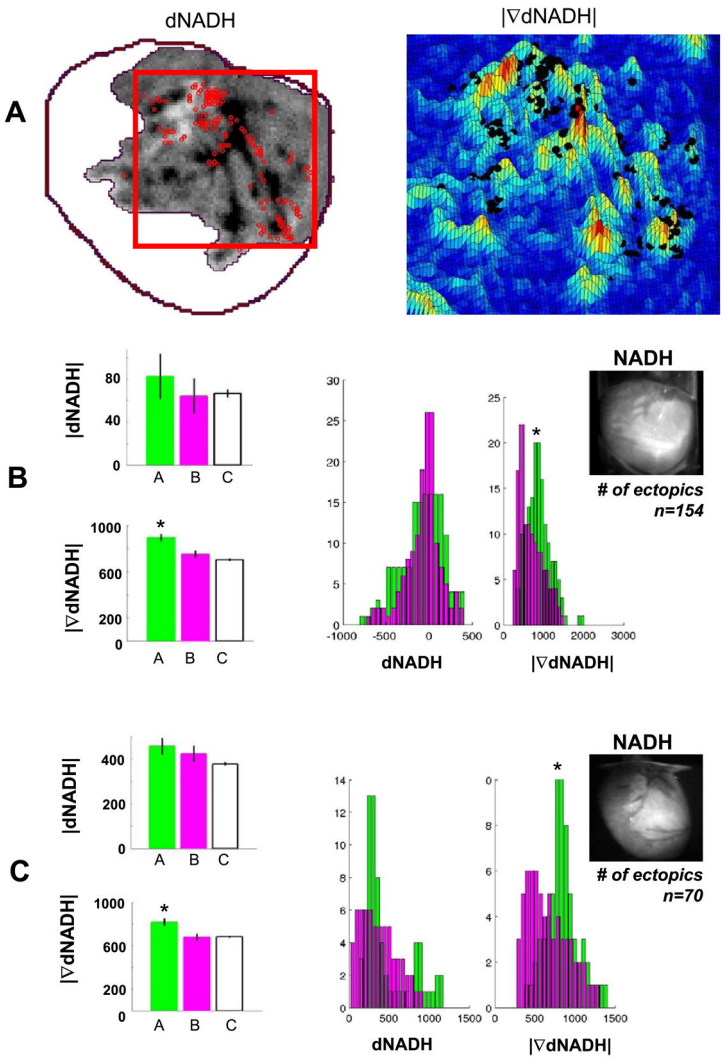

Fig. 4.

Locations of ectopic sources correlate with high spatial gradients of the change in NADH fluorescence caused by low-flow reperfusion. *A: left*, dNADH for the affected vascular bed. Red dots show sites of ectopic beats that were identified from optical mapping data; *right*, pseudocolored surface of |∇dNADH| for dNADH in the red box shown on *left*. The sites of ectopic beats shown on *left* are plotted again as black dots. *B* and *C*: dNADH and |∇dNADH| datasets from two studies for sites of ectopic sources (*set A*, green), random sites (*set B*, magenta), and all sites (*set C*, white). Average values and standard errors are plotted on the *left*. Dataset histograms for *sets A* and *B* are plotted on the *right*. *Significant differences between the other datasets shown ($P < 0.001$). *Top right inset*: an NADH image before low-flow reperfusion.